Novel photosystem involving protonation and deprotonation processes modelled on a PYP photocycle†

Takashi Matsuhira, Kazuki Tsuchihashi, Hitoshi Yamamoto,* Taka-aki Okamura and Norikazu Ueyama

Received 1st May 2008, Accepted 30th May 2008
First published as an Advance Article on the web 1st July 2008
DOI: 10.1039/b807417h

The synthesis of novel *ortho*-coumaric acid derivatives, with an amide group linked with an olefin moiety, which introduced photoinduced switching of the intramolecular hydrogen bonds is presented. An intramolecular OH···O=C hydrogen bond formed in a *Z*-phenol compound was switched to an intramolecular NH···O hydrogen bond in *Z* phenolate state *via* deprotonation. The pK_a value of the *Z*-phenol derivative was lower than that of *E*-phenol, and a novel photocycle system involving protonation and deprotonation processes was achieved.

Introduction

Photoactive yellow protein (PYP) is one of the photoreceptor proteins involved in the negative phototactic response of purple photosynthetic bacteria.[1] The photocycle of PYP around the chromophore indicates that hydrogen bonds between phenolate oxygen and hydroxyl moieties of Glu 46 or Tyr 42, which were formed in the ground state, were interrupted by *E*–*Z* photoisomerization of a *para*-coumaric acid framework, accompanying the protonation and deprotonation processes of the phenol moiety (Fig. 1). Rearrangement of the hydrogen bond network around the active site is believed to play a substantial role in regulating the reactivity of enzymatic reactions not only in PYP, but also in other native proteins, such as hydrolytic enzymes.[2] These proteins induce dynamic changes in the overall protein structure—triggered by external stimulation, such as substance binding, pH change, temperature change, or photoillumination—resulting in a switching of the hydrogen bond network. We propose that, by controlling the distance between the hydrogen bond donor and acceptor, the small molecules that switch their conformation by external stimulation will achieve switching of the intramolecular hydrogen bonding artificially (Fig. 2).

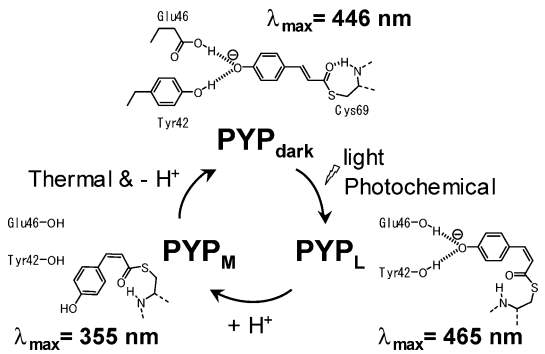

Fig. 1 Photocycle of the photoactive yellow protein (PYP).

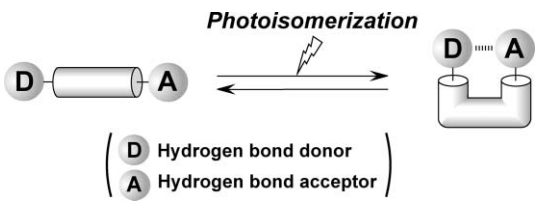

Fig. 2 Switching of the intramolecular distance of hydrogen bond donor and acceptor, by external stimulation.

Photoisomerization is one of the most promising strategies to drive these changes, enabling molecular structures to be controlled in an elegant way. Recently, much attention has been focused on the isomerization reaction of photochromic compounds as photoinduced switching devices.[3] For example, researchers have investigated the effect of intramolecular NH···N or NH···O hydrogen bonds in *Z* form on the *E*–*Z* photoisomerization of the C=C double bond,[4] as well as the pK_a change of phenol or carboxylic acid derivatives caused by the switching of conjugation through photoisomerization.[5]

Previously, we have proposed that a hydrogen bond between an amide NH and an oxyanion, such as carboxylate and phenolate, stabilizes and decreases the nucleophilicity of the anions and lowers the pK_a values of the corresponding acids.[6] We reported carboxylic acid derivatives that could switch the intramolecular distance between carboxylic oxygen and amide groups through *E*–*Z* photoisomerization, and revealed that the intramolecular NH···O hydrogen bond formed in the carboxylate lowers the pK_a value of the corresponding carboxylic acid.[7] In this study, we designed *ortho*-coumaric acid derivatives (*E*-**1**/*Z*-**1**, *E*-**2**/*Z*-**2**), both of which have an amide group linked with a photoinduced olefin moiety (Scheme 1). These compounds are expected to

Department of Macromolecular Science, Graduate School of Science, Osaka University, 1-1 Machikaneyama-cho, Toyonaka, Osaka, 560-0043, Japan. E-mail: jin@chem.sci.osaka-u.ac.jp; Fax: +81-6-6850-5474; Tel: +81-6-6850-5451

† Electronic supplementary information (ESI) available: Cif data of *E*-**1** and *Z*-**1**, UV–vis spectrum changes by photoisomerization, and COSY correlations in the NOESY spectrum. CCDC reference numbers 684897 and 684898. For ESI and crystallographic data in CIF or other electronic format see DOI: 10.1039/b807417h

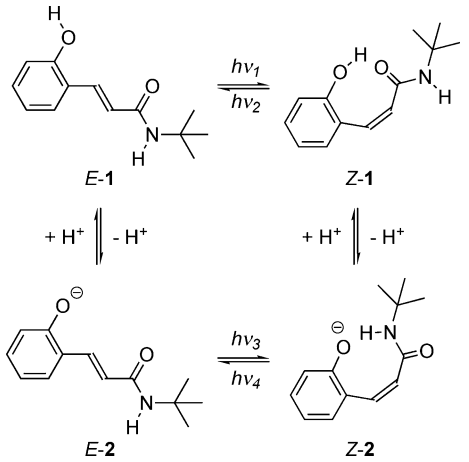

Scheme 1 Photoisomerization equilibriums of cinnamic acid derivatives *E*-**1**/*Z*-**1** and *E*-**2**/*Z*-**2**.

have an intramolecular OH · · · O=C hydrogen bond in *Z*-**1** and an intramolecular NH · · · O hydrogen bond in *Z*-**2**, forming eight-membered ring structures. And they are expected to construct an artificial cycle that involves protonation and deprotonation processes, as in the PYP photocycle. A *tert*-butyl moiety was introduced for the purpose of protecting the amide NH moiety from intermolecular interaction so as to support the construction of an intramolecular NH · · · O hydrogen bond.

Results and discussion

Synthesis

The synthetic method is shown in Scheme 2. *E*-**1** was synthesized through dicyclohexyl carbodiimide (DCC) coupling of *ortho*-coumaric acid and *tert*-butyl amine. *Z*-**1** was isolated from the photoreaction mixture by recrystallization. *E*-**2** and *Z*-**2** were prepared through a countercation exchange reaction of the corresponding phenol derivatives (*E*-**1** and *Z*-**1**) with tetraethylammonium hydroxides.

Molecular structures in the solid state

To confirm the molecular structures in the solid state, X-ray crystallography was used. The crystal structures of *E*-**1** and *Z*-**1** are shown in Fig. 3. The crystal data are shown in the experimental section. All non-hydrogen atoms were refined anisotropically. The coordinates of OH and NH protons were refined by using fixed thermal factors, and the other protons were placed in calculated positions. The intermolecular O01 · · · O′02 (2.645[2] Å) and O01 · · · N″1 (3.099[3] Å) distances of *E*-**1** permitted hydrogen bond formation; these intermolecular NH · · · O and OH · · · O=C hydrogen bonds are thought to stabilize the packing structure of *E*-**1** [O′02 indicates an O02 atom at an equivalent position ($-x + 1$, $y + 1/2$, $-z + 1/2$), and N″1 indicates an N1 atom at an equivalent position ($x + 1/2$, y, $-z + 1/2$)]. The torsion angles of C5–C6–C7–C8 (16.5 [4]°) and C7–C8–C9–O02 (20.3[4]°) indicate that the

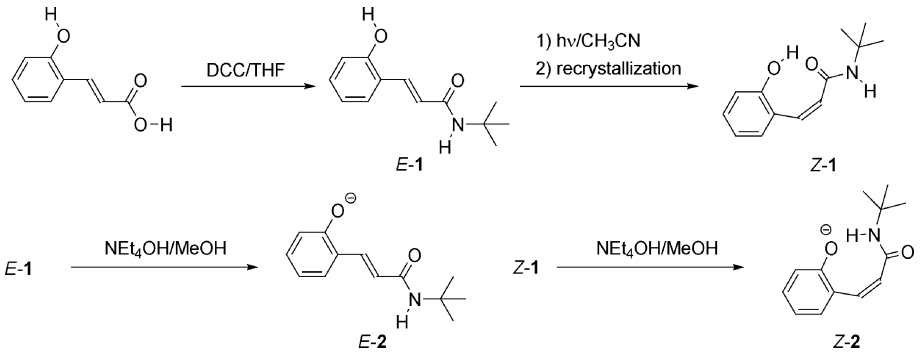

Scheme 2 Synthesis of cinnamic acid derivatives *E*-**1**, *Z*-**1**, *E*-**2** and *Z*-**2**.

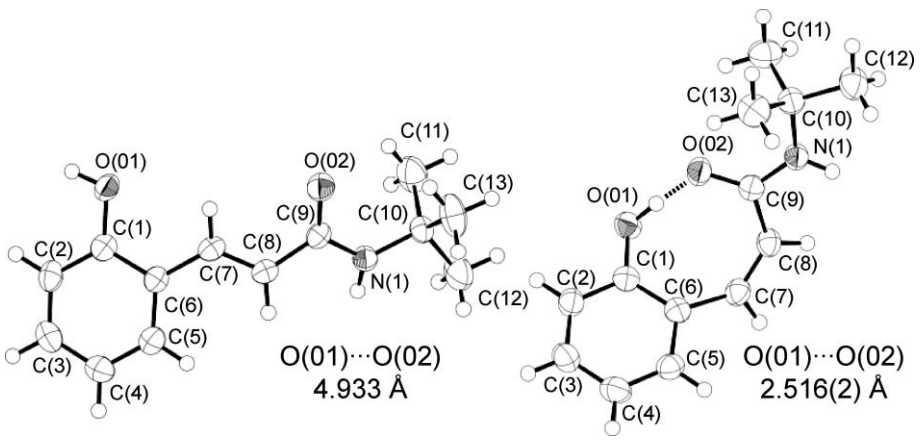

Fig. 3 Molecular structures of *E*-**1** (left) and *Z*-**1** (right), ellipsoids set as 50% probability.

ortho-coumaric frame of *E*-**1** is almost in plane; it can be inferred that the π-conjugation is extended from the phenol oxygen toward the amide carbonyl oxygen through a C=C double bond.

With *Z*-**1**, by contrast, the distances of O01 ··· O02 (2.516[2] Å) and H01 ··· O01 (1.63[2] Å) were sufficient to permit hydrogen bond formation (whereas the O01 ··· O02 distance of *E*-**1** was 4.933 Å). The O01–H01–O03 angle of *Z*-**1** (164[2]°) is suitable to cause hydrogen bonding. These results indicate that *Z*-**1** has an intramolecular OH ··· O=C hydrogen bond, forming an eight-membered ring structure in the solid state. The intermolecular O1 ··· N′1 distance (2.971 Å) of *Z*-**1** permitted intermolecular hydrogen bond formation; and was thought to stabilize the packing structure of *Z*-**1** (N′1 indicates an N1 atom at an equivalent position). The torsion angles of C5–C6–C7–C8 (−137.4[3]°) and C7–C8–C9–O02 (−27.0 [4]°) are so large that π-conjugation extended in *E*-**1** is interrupted in *Z*-**1**.

Molecular structures in solution

The molecular structures of isolated isomers in solution were determined by ^{1}H NMR spectroscopy. The ^{1}H NMR spectra of *E*-**1**, *E*-**2**, *Z*-**1**, and *Z*-**2** in acetonitrile-d_3 at 303 K are shown in Fig. 4. All signals are assigned by nuclear Overhauser effect (NOE) and decoupling method. *E*–*Z* configurations of these compounds were confirmed by the $^3J_{HH}$ values of the olefin protons. Generally speaking, the $^3J_{HH}$ coupling constant of the olefin protons is about 15 to 16 Hz in the *trans* position, and is about 12 to 13 Hz in the *cis* position. The observed $^3J_{HH}$ values of the olefin protons of *E*-**1** and *E*-**2** were 15.8 and 15.5 Hz, respectively, and those of *Z*-**1** and *Z*-**2** were 13.0 Hz. This coincides with the typical values of the *trans* and *cis* olefin protons. The configurations of the compounds before irradiation were confirmed to be the *E* form, and the photoproducts were confirmed to be the *Z* form. The chemical shifts of the OH signals of the phenol compounds at 303 K were 7.33 ppm in *E*-**1** and 9.87 ppm in *Z*-**1** (Fig. 4). The substantial downfield shift ($\Delta\delta = 2.54$ ppm) suggests that *Z*-**1** forms an OH ··· O=C hydrogen bond in acetonitrile-d_3 solution. The temperature dependency values of the OH signal chemical shifts of *E*-**1** and *Z*-**1** are −7.2 and −7.5 ppb K^{-1}, respectively, in the range of 233 to 303 K. These results indicate a hydrogen bond formation of the phenol OH moiety in *Z*-**1**, including not only an intramolecular interaction but also an intermolecular interaction. The chemical shifts of the amide NH signals of phenolates at 303 K were 6.11 ppm in *E*-**2** and 9.59 ppm in *Z*-**2** (Fig. 4). The temperature dependency value of the amide NH chemical shift of *Z*-**2** is 1.2 ppb K^{-1} (in the range of 233 to 303 K), whereas that of *E*-**2** is −5.4 ppb K^{-1} (263 to 333 K). The substantial downfield shift ($\Delta\delta = 3.48$ ppm) and the decrease of the temperature coefficient of the NH proton signal suggest that *Z*-**2** forms an intramolecular NH ··· O hydrogen bond in acetonitrile-d_3 solution.

The nuclear Overhauser enhancement spectroscopy (NOESY) spectra were measured to gain information about the molecular structure in solution (Fig. 5). A negative NOE correlation between NH and H1 was observed in *E*-**1**, whereas no NOE signal was observed between NH and H2 (Fig. 5a). Also, the correlation of H1–H3 was stronger than that of H2–H3. These results indicate that *E*-**1**, in acetonitrile-d_3 solution, seems to take the conformation shown in Fig. 5a, in which the amide carbonyl

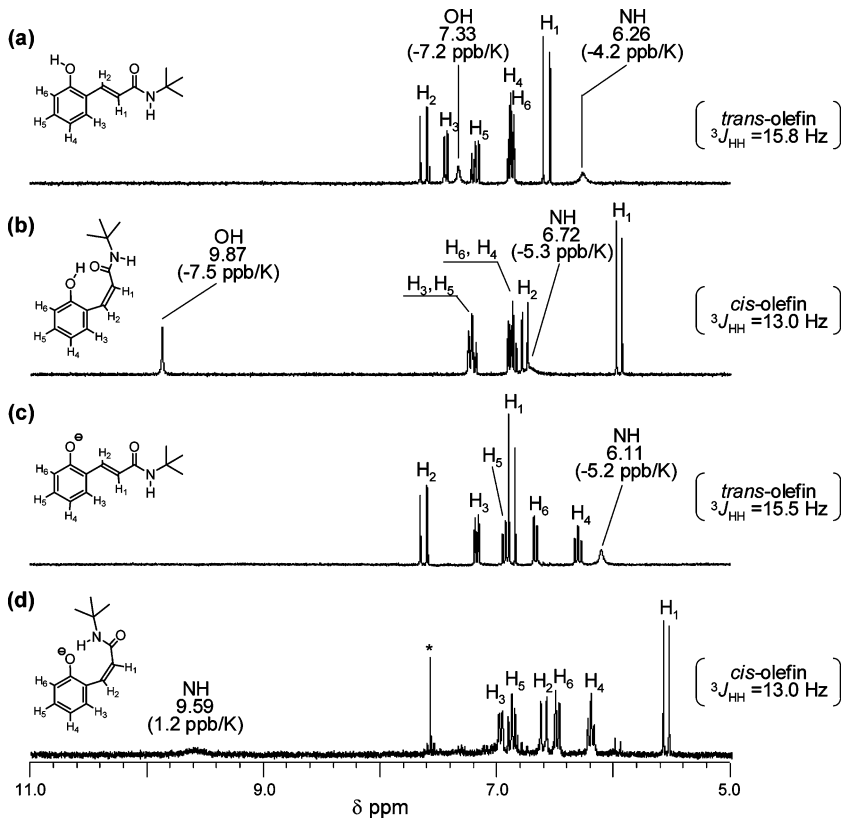

Fig. 4 ^{1}H NMR spectra of (a) *E*-**1**, (b) *Z*-**1**, (c) *E*-**2** and (d) *Z*-**2**, 5 mM in acetonitrile-d_3 at 303 K.

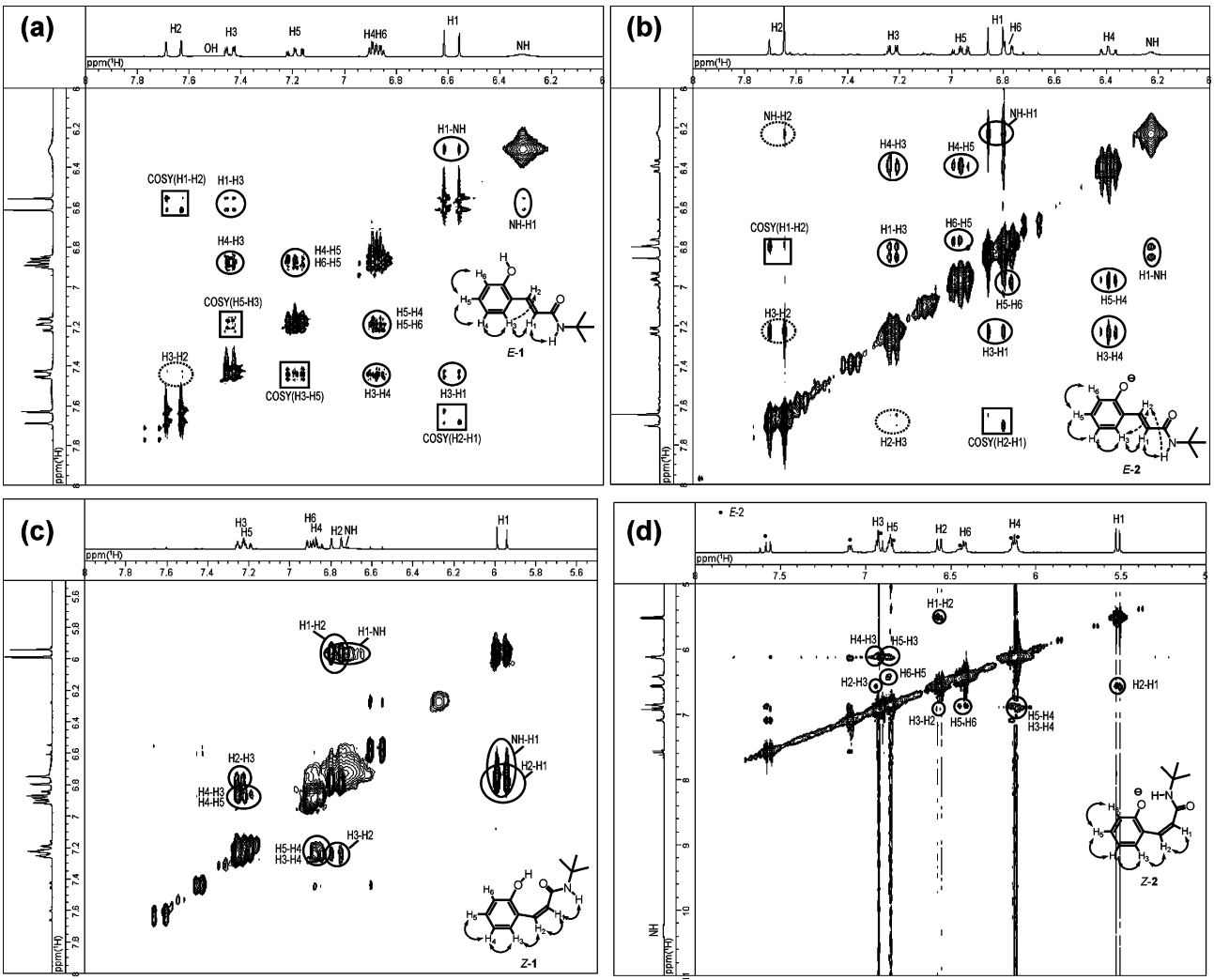

Fig. 5 NOESY spectra of (a) *E*-**2** and (b) *Z*-**2**, 5 mM in acetonitrile-d_3 at 303 K.

orients toward the olefin moiety (s-*cis* form) and the hydroxyl moiety orients in the opposite direction of the olefin moiety (s-*trans* form). This structure of *E*-**1** is consistent with the solid structure obtained with X-ray crystallography (Fig. 3). The characteristic positive–negative correlation patterns of H1–H2 and H5–H3 are predicated to the correlated signal (COSY signal) caused by spin coupling (ESI†). The correlation of the hydroxyl OH proton was not observed but exchange signal (EXSY signal) with water protons was observed. The NOE pattern of *E*-**2** was almost the same as that of *E*-**1**, and *E*-**2** seems to take the structure shown in Fig. 5b in acetonitrile-d_3 solution. The correlation of H1–H2 in *E*-**2** was the COSY signal as well as that in *E*-**1** (ESI†).

In *Z*-**1**, a negative NOE correlation between H1 and H2 was observed (Fig. 5c). This correlation is characteristically seen in the *cis* configuration of the olefin protons; therefore the configuration of *Z*-**1** is determined to be definitely in the *Z* form. Correlations of NH–H1 and H2–H3 were observed, and no NOE signal was observed around the OH protons. These results indicate that *Z*-**1** seems to adopt the structure shown in Fig. 5c, with the hydroxyl proton in close proximity to the amide carbonyl oxygen, and is able to form an intramolecular OH $\cdots$ O=C hydrogen bond. In *Z*-**2**, an NOE correlation of NH–H1, which was characteristically observed in *Z*-**1**, was not seen (Fig. 5d). Additionally, the correlation of H2–H3 was observed. These results can be ascribed to the flipping of the amide plane by switching of the intramolecular hydrogen bond from OH $\cdots$ O=C to NH $\cdots$ O^-, accompanying the deprotonation of the phenol moiety (Scheme 3).

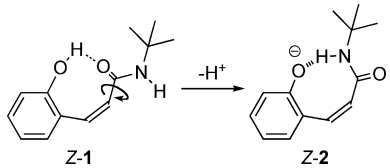

Scheme 3 Flipping of the amide plane with the deprotonation of *Z*-**1**.

Direct photoisomerization

Fig. 6 shows the UV–visible (UV–vis) spectra of isolated compounds (*E*-**1**, *E*-**2**, *Z*-**1**, *Z*-**2**), in acetonitrile at 303 K. The wavenumbers of maximum absorbance (λ_{max}) in the phenolate derivatives (*E*-**2**, *Z*-**2**) were longer than those in the corresponding phenol derivatives (*E*-**1**, *Z*-**1**). The red shift of λ_{max} can be ascribed

Table 1 *E*–*Z* ratios in the photostationary state (PSS) at various irradiation wavelengths

	Irradiation wavelength			
	313 nm	365 nm	405 nm	436 nm
E-**1**–*Z*-**1**	11 : 89	18 : 82	No reaction	No reaction
E-**2**–*Z*-**2**	51 : 49	13 : 87	16 : 84	30 : 70

to electron delocalization in the phenolate derivatives. The UV–vis spectra in Fig. 6 indicate that the mercury lamp wavelength emissions for direct photoexcitation are 313 and 365 nm in the phenol derivatives, and 313, 365, 405, and 436 nm in the phenolate derivatives, without using any photosensitizer. Following photoirradiation, *E*–*Z* isomerization progressed without any effective side reactions (ESI†). The *E*–*Z* ratio in the photostationary state (PSS) depends on the irradiation wavelength. The ratios in PSS at various wavelengths are shown in Table 1. At 313-nm irradiation, in PSS, the products were rich in *Z* configuration phenol derivatives (*E*-**1**–*Z*-**1** = 11 : 89), whereas the amounts of *E* and *Z* phenolate derivatives in PSS were almost equal (*E*-**2**–*Z*-**2** = 51 : 49). At 365-nm irradiation, both phenol and phenolate derivatives generate *Z* isomers rather than *E* isomers (*E*-**1**–*Z*-**1** = 18 : 82, *E*-**2**–*Z*-**2** = 13 : 87). The phenolate derivatives generate the *Z* compound in PSS with irradiation at 405 nm (*E*-**2**–*Z*-**2** = 16 : 84) and at 436 nm (*E*-**2**–*Z*-**2** = 30 : 70), whereas no reaction occurs with the phenol derivatives because *E*-**1** and *Z*-**1** have no absorption at these wavelengths. The phenolate derivatives progress through a reversible photoisomerization: *E* to *Z* conversion by 405-nm irradiation, and *Z* to *E* reversal by 313-nm irradiation (ESI†).

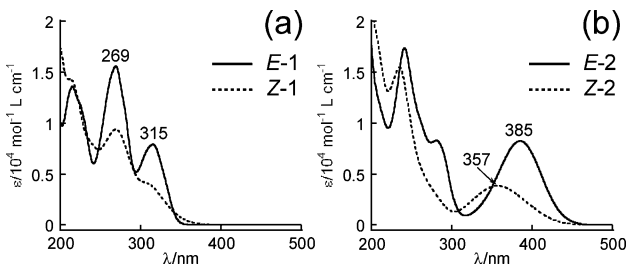

Fig. 6 UV–vis spectra of *E*-**1**, *Z*-**1** and *E*-**2**, *Z*-**2**, 1 mM in acetonitrile at 293 K.

Acidity change through photoisomerization

pK_a values of *E*-**1** and *Z*-**1** were measured by potentiometric titration traced with UV–vis spectra in a 10% lauryl ether aqueous micellar solution at 303 K. UV–vis spectra changes caused by the addition of aqueous sodium hydroxide solution (0.100 mol L^{-1}) are shown in Fig. 7. As the pH value increased, the absorbances of phenol derivatives (323 nm in *E*-**1** and 311 nm in *Z*-**1**) decreased, and those of phenolate derivatives (380 nm in *E*-**2** and 357 nm in *Z*-**2**) increased. The titration curves are shown in Fig. 8. The Henderson–Hasselbalch equation of acid dissociation in a buffering region shows that the pK_a value is equal to the pH value when the concentration of phenolate matches that of phenol.

$$[HA] \rightleftharpoons [H^+] + [A^-]$$

〈*Henderson-Hasselbalch* equasion〉

$$pH = pK_a + \log [A^-] - [AH]$$

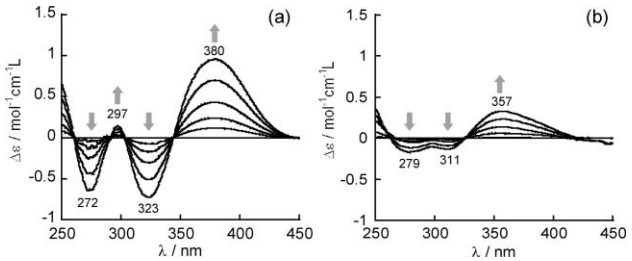

Fig. 7 UV–vis spectra changes for phenol compounds, by the addition of aqueous sodium hydroxide solution, (a) *E*-**1** and (b) *Z*-**1**, 5 mM in 10% lauryl ether aqueous micellar solution at 303 K.

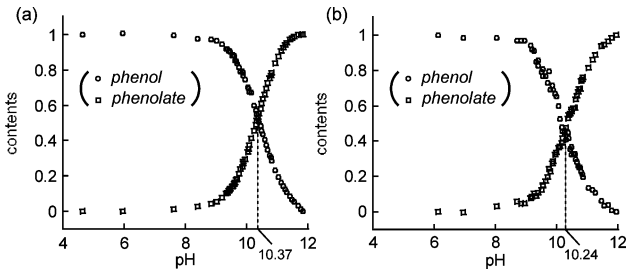

Fig. 8 Titration curves of (a) *E*-**1** and (b) *Z*-**1**.

Thus the pH value at the intersection of the titration curves of phenol and phenolate in Fig. 8 stimulates the pK_a value of the corresponding phenol derivatives. The pK_a value of *Z*-**1** was 10.24, which has a shift that is 0.13 units lower than that of *E*-**1** (10.37). We propose that the stabilization of the *Z* phenolate derivative (*Z*-**2**) by the formation of an intramolecular NH···O hydrogen bond decreases the pK_a value of the *Z* phenol derivative (*Z*-**1**). Fig. 9 shows a comparison of the titration curves of phenol derivatives. In the pH region around the pK_a values of *E*-**1** and *Z*-**1** (a buffering region), the *E* compound was protonated and the *Z* compound was deprotonated, preferentially. We propose that photoisomerization of a compound synthesized in this pH region will achieve control over the protonation and deprotonation of the phenolic hydroxyl moiety.

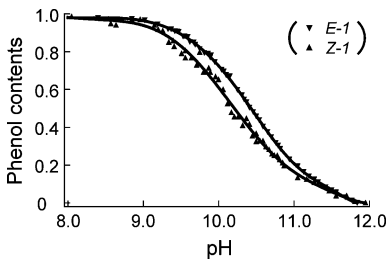

Fig. 9 Comparison of titration curves of *E*-**1** and *Z*-**1**; ratios of phenol components depend on pH.

Proposed photocycle

The decrease of the pK_a value in a *Z* phenol compound, and the differences in *E*–*Z* ratios between phenol and phenolate derivatives in PSS at 313-nm irradiation, indicate that the novel photocycle system is probably constructed like the PYP photocycle, involving protonation and deprotonation processes (Scheme 4). In this photocycle, *E* phenol derivatives photoisomerize toward

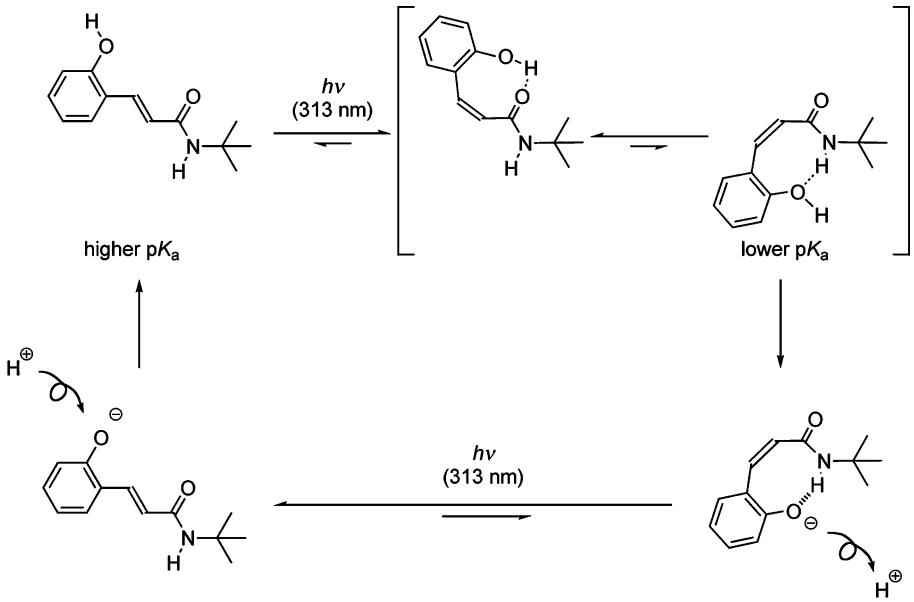

Scheme 4 Proposed photocycle.

Z phenols at a UV irradiation wavelength of 313 nm. Then, deprotonation progresses because of the decrease of the pK_a value in the *Z* phenol. The *Z* phenolate photoisomerizes towards the *E* isomer at the same UV irradiation wavelength (313 nm), and the *E* phenolate returns to the initial state by a protonation process. Through a series of repetitions of this photocycle, phenolate was protonated far from the amide moiety, and phenol was deprotonated near the amide moiety. This indicates proton transport from the far side to the near side of the amide moiety, using light energy as a driving force. It represents the achievement of a light-driven proton pumping system using an artificial small molecule.

Conclusion

In this work, the authors designed a novel photocycle system, consisting of phenol *E*-**1**/*Z*-**1** and phenolate *E*-**2**/*Z*-**2** derivatives, that was modelled on the PYP photocycle. *Z*-**1** was shown to form an intramolecular OH···O=C hydrogen bond both in acetonitrile-d_3 solution and in the solid state, and *Z*-**2** was shown to form an intramolecular NH···O hydrogen bond in acetonitrile-d_3 solution. The *ortho*-coumaric acid moiety has an extended π-conjugation in phenolate, thus a red shift of the absorption maximum was observed. Because of the difference in the absorption wavelength, phenol and phenolate have different *E*–*Z* ratios at the same UV light irradiation wavelength. UV light irradiation at a wavelength of 313 nm generates the *Z* form in phenol and generates the *E* form in phenolate, preferentially. The reversion rate led to an almost equal amount of both compounds (*E*–*Z* = 51 : 49). To improve the reversion rate, the substitution of the conjugated aromatic moiety would be effective to control the compounds' absorbance maxima. The pK_a value of the phenol compound was lowered in the *Z* compound by stabilizing the *Z* phenolate with formation of an intramolecular NH···O hydrogen bond. The change of the *E*–*Z* ratio in phenol and phenolate, and the decrease of the pK_a value in the *Z* phenol compound, indicate that the artificial photocycle was constructed like the PYP photocycle, which involves protonation and deprotonation processes.

Experimental

General procedures

All manipulations involving air- and moisture-sensitive compounds were carried out by the use of a standard Schlenk technique under an argon atmosphere. *E*-*ortho*-coumaric acid, 25% tetraethylammonium bydroxide in methanol solution were purchased from Tokyo-Kasei Co. Dicyclohexylcarbodiimide was purchased from Peptide Institute, Inc. Dichloromethane was distilled over CaH_2. Methanol, tetrahydrofuran, diethylether, *n*-hexane, and acetonitrile were distilled over CaH_2 and dried over molecular sieves (3Å).

Physical measurements

^{1}H (270 MHz) NMR spectra were measured on a JEOL JNM-GSX270 spectrometer. ^{13}C (100, 120 MHz) NMR spectra were measured on a JEOL JNM-GSX400 spectrometer, and on a Varian UNITYplus 600 MHz spectrometer. NOESY spectra were measured on a JEOL JNM-GSX400 spectrometer and Varian UNITYplus 600 MHz spectrometer. The ^{1}H NMR spectra were referenced to tetramethylsilane protons at δ 0.00. The ^{13}C NMR spectra were referenced to the methyl carbon of acetonitrile-d_3 at δ 1.30. UV–vis spectra was measured on a Shimazu UV-3100PC and Ocean Optics Inc. TP300-UV/VIS spectrometers. Elemental analysis was performed at the Elemental Analysis Center, Faculty of Science, Osaka University. All melting points of the compounds were measured on a micro melting point apparatus from YANAGIMOTO Co. ESI-MS measurements were performed on a Finnigan MAT LCQ ion trap mass spectrometer. FT-IR spectra were measured on a JASCO FT/IR-8300 spectrometer; the FT-IR measurement was performed in KBr glass cell with

nujol or with solvent. pK_a measurements were performed using a potentiometric titration in 10 mM micellar solution at 298 K with a Metrohm 716 DMS titrino combined with a Metrohm 728 stirrer and a saturated calomel LL micro pH glass electrode. The saturated calomel micro glass electrode was calibrated with a 0.05 M $KHC_8H_4O_4$ buffer (pH = 4.01) and a 0.0025 M KH_2PO_4 buffer (pH = 6.87) at 303 K. The potentiometric titrations were performed three times. pK_a values were estimated by an average value of each measurement.

Preparation of (*E*)-*N*-*tert*-butyl-3-(2-hydroxyphenyl) acrylamide (*E*-1)

To a 1 L tetrahydrofuran solution of *E*-*ortho*-coumaric acid (2.01 g, 12.2 mmol) and *tert*-butylamine (2.6 mL, 24.4 mmol) was added dicyclohexylcarbodiimide (DCC, 4.44 g, 24.4 mmol). The white suspension was stirred at room temperature for 2 days. The solvent was removed under reduced pressure to obtain a white solid. The solid was dissolved in 100 mL of 0.8 mol L^{-1} aqueous sodium hydroxide solution. The yellow solution was moved to a dropping funnel and washed with 150 mL of ethyl acetate–diethyl ether (1 : 1, v/v). The organic layer was extracted again by 0.8 M aqueous sodium hydroxide solution three times. The combined aqueous layers were washed with 100 mL of *n*-hexane. Whilst cooling in an ice bath, the aqueous layer was acidified by aqueous sulfuric acid solution (pH 6–7). The orange solution turned to a white suspension. The mixture was extracted with ethyl acetate–diethyl ether (1 : 1, v/v) three times. The organic layer was washed with 4% aqueous sodium bicarbonate solution three times. The organic layer was dried over anhydrous magnesium sulfate, and the solvent was removed under reduced pressure. The white powder was recrystallized from hot acetonitrile to obtain colorless crystals (1.25 g 46.8%). Mp 229–230 °C; (Found: C, 71.14; H, 7.90; N, 6.53. Calc. for $C_{13}H_{17}NO_2$: C, 71.21; H, 7.81; N, 6.39%); ν_{max}(in nujol mull)/cm^{-1} 3357 (NH), 3130–3047 (OH), and 1657 (C=O); ν_{max}(in acetonitrile solution)/cm^{-1} 3380 (NH), and 1672 (C=O); δ_H(270 MHz; acetonitrile-d_3) 1.36 (s, 9H; *tert*-butyl), 6.26 (br s, 1H; NH), 6.58 (d, ^3J(H,H) = 15.8 Hz, 1H; olefin), 6.87 (dd, ^3J(H,H) = 8.2 Hz, ^4J(H,H) = 1.2 Hz, 1H; aryl), 6.88 (dt, ^3J(H,H) = 8.2 Hz, ^4J(H,H) = 1.2 Hz, 1H; aryl), 7.18 (dt, ^3J(H,H) = 8.2 Hz, ^4J(H,H) = 1.2 Hz, 1H; aryl), 7.33 (br s, 1H; OH), 7.44 (dd, ^3J(H,H) = 8.2 Hz, ^4J(H,H) = 1.2 Hz, 1H; aryl), 7.63 ppm (d, ^3J(H,H) = 15.8 Hz, 1H; olefin); δ_C(100 MHz; acetonitrile-d_3) 29.0, 51.7, 117.0, 121.2, 123.4, 124.2, 129.5, 131.4, 135.1, 156.6, and 166.5 ppm; *m*/*z* (ESI) 218.3 ([M − H]$^-$ requires 218.1), 220.1 ([M + H]$^+$ requires 220.1), 242.2 ([M + Na]$^+$ requires 242.1), 461.0 ([2M + Na]$^+$ requires 461.2); pK_a = 9.84 (10 mM in 10% aqueous micellar solution of Triton® X-100).

Preparation of (*Z*)-*N*-*tert*-butyl-3-(2-hydroxyphenyl) acrylamide (*Z*-1)

(*E*)-*N*-*tert*-Butyl-3-(2-hydroxyphenyl) acrylamide (*E*-**1**, 441.2 mg, 2.01 mmol) was dissolved in 50 mL of acetonitrile. UV-light was irradiated on the solution for 400 minutes. The solvent was removed under reduced pressure. The residue was reprecipitated from diethyl ether–*n*-hexane. A white precipitate was collected by filtration and was suspended in ice-cooled chloroform. The suspension was filtered and the filtrate was concentrated under reduced pressure. The obtained pale yellow powder was recrystallized from ethyl acetate–*n*-hexane to obtain colorless crystals (154.4 mg, 35%). ν_{max}(in acetonitrile solution)/cm^{-1} 3360 (NH), and 1645 (C=O); δ_H(270 MHz; acetonitrile-d_3) 1.32 (s, 9H; *tert*-butyl), 5.97 (d, ^3J(H,H) = 13.0 Hz, 1H; olefin), 6.72 (br s, 1H; NH), 6.77 (d, ^3J(H,H) = 13.0 Hz, 1H; olefin), 6.87 (dt, ^3J(H,H) = 7.5 Hz, ^4J(H,H) = 1.2 Hz, 1H; aryl), 6.89 (dd, ^3J(H,H) = 7.5 Hz, ^4J(H,H) = 1.2 Hz, 1H; aryl), 7.22 (dt, ^3J(H,H) = 7.5 Hz, ^4J(H,H) = 1.2 Hz, 1H; aryl), 7.23 (dd, ^3J(H,H) = 7.5 Hz, ^4J(H,H) = 1.2 Hz, 1H; aryl), 9.87 ppm (br s, 1H; OH); δ_C(100 MHz; acetonitrile-d_3) 28.7, 52.6, 120.0, 120.7, 123.9, 125.8, 131.3, 133.2, 136.7, 156.7, and 168.8 ppm; *m*/*z* (ESI) 220.1 ([M + H]$^+$ requires 220.1), 460.9 ([2M + Na]$^+$ requires 461.2); pK_a = 9.70 (10 mM in 10% aqueous micellar solution of Triton® X-100).

Preparation of [tetraethyl-ammonium] 2-((*E*)-2-(*tert*-butylcarbamoyl)vinyl) phenolate (*E*-2)

(*E*)-*N*-*tert*-Butyl-3-(2-hydroxyphenyl) acrylamide (*E*-**1**, 100.9 mg, 0.46 mmol) was dissolved in 1 mL of methanol. To the solution was added 25% tetraethylammonium hydroxide solution in methanol (0.25 mL, 0.41 mmol). The solution was stirred for 2 hours and the solvent was removed under reduced pressure. The residue was washed with 10 mL of diethyl ether twice. The powder was recrystallized from acetonitrile–diethyl ether to obtain a yellow crystalline solid. ν_{max}(in acetonitrile solution)/cm^{-1} 3386 (NH), and 1661 (C=O); δ_H(270 MHz; acetonitrile-d_3) 1.20 (t, ^3J(H,H) = 7.3 Hz, 12H; NEt_4), 1.35 (s, 9H; *tert*-butyl), 3.15 (q, ^3J(H,H) = 7.3 Hz, 8H; NEt_4), 6.11 (s, 1H; NH), 6.31 (dt, ^3J(H,H) = 7.3 Hz, ^4J(H,H) = 1.2 Hz, 1H; aryl), 6.67 (dd, ^3J(H,H) = 7.3 Hz, ^4J(H,H) = 1.2 Hz, 1H; aryl), 6.88 (d, ^3J(H,H) = 15.5 Hz, 1H; olefin), 6.92 (dt, ^3J(H,H) = 7.3 Hz, ^4J(H,H) = 1.2 Hz, 1H; aryl), 7.18 (dd, ^3J(H,H) = 7.3 Hz, ^4J(H,H) = 1.2 Hz, 1H; aryl), 7.62 ppm (d, ^3J(H,H) = 15.5 Hz, 1H; olefin); δ_C(100 MHz; acetonitrile-d_3) 7.7, 29.3, 51.0, 53.2, 85.0, 89.9, 108.4, 116.0, 122.6, 131.1, 131.7, 141.8, and 169.3 ppm; *m*/*z* (ESI) 218.3 ([M − NEt_4]$^-$ requires 218.1), 349.3 ([M + H]$^+$ requires 349.3), 335.3 ([M − Me + 2H]$^+$ requires 335.3), 321.5 ([M − Et + 2H]$^+$ requires 321.3).

Preparation of [tetraethyl-ammonium] 2-((*Z*)-2-(*tert*-butylcarbamoyl)vinyl) phenolate (*Z*-2)

(*Z*)-*N*-*tert*-Butyl-3-(2-hydroxyphenyl) acrylamide (*Z*-**1**, 100.9 mg, 0.46 mmol) was dissolved in 1 mL of methanol. To the solution was added 25% tetraethylammonium hydroxide solution in methanol (0.25 mL, 0.41 mmol). The solution was stirred for 2 hours and the solvent was removed under reduced pressure. The residue was washed with 10 mL of diethyl ether twice. The powder was recrystallized from acetonitrile–diethyl ether to obtain a yellow crystalline solid. ν_{max}(in acetonitrile solution)/cm^{-1} 1635 (C=O); δ_H(270 MHz; acetonitrile-d_3) 1.21 (t, ^3J(H,H) = 7.4 Hz, 12H; NEt_4), 1.23 (s, 9H; *tert*-butyl), 3.16 (q, ^3J(H,H) = 7.4 Hz, 8H; NEt_4), 5.57 (d, ^3J(H,H) = 13.0 Hz, 1H; olefin), 6.21 (dt, ^3J(H,H) = 7.6 Hz, ^4J(H,H) = 1.8 Hz, 1H; aryl), 6.50 (dd, ^3J(H,H) = 7.6 Hz, ^4J(H,H) = 1.8 Hz, 1H; aryl), 6.61 (d, ^3J(H,H) = 13.0 Hz, 1H; olefin), 6.89 (dt, ^3J(H,H) = 7.6 Hz, ^4J(H,H) = 1.8 Hz, 1H; aryl), 6.98 (dd, ^3J(H,H) = 7.6 Hz, ^4J(H,H) = 1.8 Hz, 1H; aryl), 9.58 ppm (br s, 1H; NH); δ_C(120 MHz; acetonitrile-d_3) 7.7, 15.6,

29.0, 53.1, 96.6, 123.6, 125.6, 130.1, 131.1, 131.3, 135.0, 161.8, and 168.1 ppm; *m/z* (ESI) 218.5 ($[M - NEt_4]^-$ requires 218.1), 349.3 ($[M + H]^+$ requires 349.3), 335.3 ($[M - Me + 2H]^+$ requires 335.3), 321.5 ($[M - Et + 2H]^+$ requires 321.3).

Crystallographic data collection and structure determination of *E*-1 and *Z*-1

Suitable single crystals of *E*-**1** and *Z*-**1** were mounted on a fine nylon loop with nujol and immediately frozen at 200 ± 1 K. All measurements were performed on a Rigaku RAXIS-RAPID Imaging Plate diffractometer with graphite monochromated MoKα radiation (λ = 0.71075 Å). The structures were solved by direct method (SIR 92)[8] and the following refinements were performed using the SHELXL-97[9] and teXsan crystallographic software packages. All non-hydrogen atoms were refined anisotropically. The coordinates of OH and NH protons were refined by using fixed thermal factors, and the other protons were placed in calculated positions. Crystal data for $C_{13}H_{17}NO_2$ (*E*-**1**): 0.35 × 0.30 × 0.02 mm^3, orthorhombic, *Pbca* (#61), a = 12.940(5) Å, b = 9.252(5) Å, c = 20.60(1) Å, V = 2466(3) Å^3, Z = 8, ρ_{calcd} = 1.181 g cm^{-3}, μ (MoK$_\alpha$) = 0.79 cm^{-1}, M_w = 219.28. Total number of reflections measured 23376, unique reflections 21726 (R_{int} = 0.174), final R indices: R_1 = 0.058, wR_2 = 0.128 for all data. GOF (F^2) = 1.03. Crystal data for $C_{13}H_{17}NO_2$ (*Z*-**1**): 0.40 × 0.35 × 0.08 mm^3, monoclinic, $P2_1/c$ (#14), a = 11.000(6) Å, b = 12.346(16) Å, c = 9.398(7) Å, β = 103.58(2)°, V = 1240(1) Å^3, Z = 4, ρ_{calcd} = 1.174 g cm^{-3}, μ (MoK$_\alpha$) = 0.79 cm^{-1}, M_w = 219.28. Total number of reflections measured 11695, unique reflections 11384 (R_{int} = 0.089), final R indices: R_1 = 0.070, wR_2 = 0.129 for all data. GOF (F^2) = 1.04.†

UV-light irradiation technique for UV–vis and ^{1}H NMR spectrum measurements

A Xe/Hg lamp (MUV-202U, Moritex Co.) was used for 313 nm UV-light irradiation. UV-light was filtered through 6784-t01.uv1 (Asahi tech.) to select the 313-nm emission line of Hg gas. For 365-, 405-, and 436-nm irradiation, filters of #43–155 FILTER INT 365NM 50.8 mm SQ, #43–156 FILTER INT 405NM 50.8 mm SQ, and #43–161 FILTER INT 436NM 50.8 mm SQ (Edmund Optics Inc.) were used respectively. The sample was dissolved in distilled solvent under an argon atmosphere and sealed in an NMR tube or a UV cell. The spectrum was measured before and after irradiation. During irradiation and spectrum measurements, the sample was always kept at the desired temperature.

Potentiometric titration traced by a UV–vis spectrum

To a solution of a phenol derivative dissolved in distilled THF was added lauryl ether, and the solution was stirred for several minutes. THF was removed under reduced pressure, and the residue was added to aqueous sodium perchlorate solution. The UV–vis spectrum and the pH value were measured at the same time, by using the reaction tracking system (ESI†). During each measurement, the sample was kept at 303 K in a temperature controlled bath.

Acknowledgements

One of the authors (T. Matsuhira) express his special thanks for the Global Education and Research Center for Bio-Environmental Chemistry (GCOE) program of Osaka University.

References

1 (*a*) G. O. Borgstahl, D. R. Williams and E. D. Getzoff, *Biochemistry*, 1995, **34**, 6278–6287; (*b*) A. Warshel, *Biochemistry*, 1981, **20**, 3167–3177; (*c*) Y. Imamoto, M. Kataoka, F. Tokunaga, T. Asahi and H. Masuhara, *Biochemistry*, 2001, **40**, 6047–6052; (*d*) Y. Imamoto, Y. Shirahige, F. Tokunaga, T. Kinoshita, K. Yoshihara and M. Kataoka, *Biochemistry*, 2001, **40**, 8997–9004; (*e*) U. K. Genick, S. M. Soltis, P. Kuhn, I. L. Canestrelli and E. D. Getzoff, *Nature*, 1998, **392**, 206–209; (*f*) M. Baca, G. E. Borgstahl, M. Boissinot, P. M. Burke, D. R. Williams, K. A. Slater and E. D. Getzoff, *Biochemistry*, 1994, **33**, 14369–14377; (*g*) M. Kim, R. A. Mathiesm, W. D. Hoff and K. J. Hellingwerf, *Biochemistry*, 1995, **34**, 12669–12672; (*h*) B. Perman, V. Srajer, Z. Ren, T. Teng, C. Pradervand, T. Ursby, D. Bourgeois, F. Schotte, M. Wulff, R. Kort, K. Hellingwerf and K. Moffat, *Science*, 1998, **279**, 1946–1950; (*i*) U. K. Genick, G. E. O. Borgstahl, Z. R. Kingham Ng, C. Pradervand, P. M. Burke, V. Srajer, T. Y. Teng, W. Schildkamp, D. E. McRee, K. Moffat and E. D. Getzoff, *Science*, 1997, **275**, 1471–1475; (*j*) A. Xie, W. D. Hoff, A. R. Kroon and K. J. Hellingwerf, *Biochemistry*, 1996, **35**, 14671–14678; (*k*) A. Xie, L. Kelemen, J. Hendriks, B. J. White, K. J. Hellingwerf and W. D. Hoff, *Biochemistry*, 2001, **40**, 1510–1517; (*l*) Y. Imamoto, K. Mihara, O. Hisatomi, M. Kataoka, F. Tokunaga, N. Bojkova and K. Yoshihara, *J. Biol. Chem.*, 1997, **272**, 12905–12908; (*m*) G. Rubinstenn, G. W. Vuister, F. A. Mulder, P. E. Dux, R. Boelens, K. J. Hellingwerf and R. Kaptein, *Struct. Biol.*, 1998, 568–570.

2 (*a*) D. P. Cruikshank, W. K. Hartmann and D. J. Tholen, *Nature*, 1985, **315**, 122–124; (*b*) M. Fujinaga, M. M. Chernaia, N. I. Tarasova, S. C. Mosimann and M. N. G. James, *Protein Sci.*, 1995, 960–972; (*c*) M. J. Millar, R. J. K. Mohano, J. Leis and A. Wlodawer, *Nature*, 1989, **337**, 576–579; (*d*) A. M. Silva, E. R. Cachau, H. L. Sham and J. W. Erickson, *J. Mol. Biol.*, 1996, **255**, 321–340; (*e*) K. Suguna, R. R. Bott, E. A. Padlan, E. Subramanian, S. Scheriff, G. H. Cohen and D. Davis, *J. Mol. Biol.*, 1987, **196**, 877–900; (*f*) A. M. Wlodawer, M. Jaskolski and B. K. Sathyanarayama, *Science*, 1989, **245**, 616–621; (*g*) B. V. A. Cheesman and D. L. Rabenstein, *J. Am. Chem. Soc.*, 1988, **110**, 6359–6364; (*h*) Z. R. Gan and W. W. Wells, *J. Biol. Chem.*, 1987, **262**, 6704–6707; (*i*) H. C. F. Hawkins, *Biochem. J.*, 1991, 335–339; (*j*) S. D. R. Katti, *Protein Sci.*, 1995, **4**, 1998–2005; (*k*) S. D. Lewis, F. A. Johnson and J. A. Shafer, *Biochemistry*, 1976, **15**, 5009–5017; (*l*) S. D. Lewis, F. A. Johnson and J. A. Shafer, *Biochemistry*, 1981, **20**, 48–51; (*m*) S. Z. P. J. Liu, W. W. Johnson, G. L. Gilliland and R. N. Armstrong, *J. Biol. Chem.*, 1992, **267**, 4296–4299; (*n*) J. L. B. Martin and J. C. A. J. Kuriyan, *Nature*, 1993, **365**, 464–468; (*o*) J. W. Nerson and T. E. Creighton, *Biochemistry*, 1994, **33**, 5974–5983; (*p*) U. Srinivasan, P. A. Mieyal and J. J. Mieyal, *Biochemistry*, 1997, **36**, 3199–3206; (*q*) C. Mattos, D. A. Giammona, G. A. Petsko and D. Ringe, *Biochemistry*, 1995, **34**, 3193–3203.

3 (*a*) M. Irie, T. Fukaminato, T. Sasaki, N. Tamai and T. Kawai, *Nature*, 2002, **420**, 759–760; (*b*) M. Irie, O. Miyatake, K. Uchida and T. Eriguchi, *J. Am. Chem. Soc.*, 1994, **116**, 9894–9900; (*c*) J. Hayakawa, A. Momotake and T. Arai, *Chem. Commun.*, 2003, 94–95; (*d*) J. Hayakawa, A. Momotake, R. Nagahata and T. Arai, *Chem. Lett.*, 2003, **32**, 1008–1009; (*e*) H. Tatewaki, T. Mizutani, J. Hayakawa, T. Arai and M. Tarazima, *J. Phys. Chem. A*, 2003, **107**, 6515–6521; (*f*) J. H. Yoo, I. Cho and S. Y. Kim, *J. Polym. Sci., Part A: Polym. Chem.*, 2004, **42**, 5401–5406; (*g*) O. Ohtani, R. Sasai, T. Adachi, I. Hatta and K. Takagi, *Langmuir*, 2002, **18**, 1165–1170; (*h*) R. Behrendt, C. Renner, M. Schenk, F. Wang, J. Wachtveitl, D. Oesterhelt and L. Moroder, *Angew. Chem., Int. Ed.*, 1999, **38**, 2771–2774; (*i*) R. Behrendt, M. Schenk, H. J. Musiol and L. Moroder, *J. Pept. Sci.*, 1999, **5**, 519–529; (*j*) S. Kobatake, S. Takami, H. Muto, T. Ishikawa and M. Irie, *Nature*, 2007, **446**, 778–781.

4 (*a*) F. D. Lewis, B. A. Yoon, T. Arai, T. Iwasaki and K. Tokumaru, *J. Am. Chem. Soc.*, 1995, **117**, 3029–3036; (*b*) T. Arai, M. Moriyama and K. Tokumaru, *J. Am. Chem. Soc.*, 1994, **116**, 3171–3172; (*c*) A. Masumoto, K. Maeda and T. Arai, *J. Phys. Chem. A*, 2003, **107**, 10039–10045; (*d*) M. Ikegami and T. Arai, *Bull. Chem. Soc. Jpn.*, 2003, **76**, 1783–1792; (*e*) M. Ikegami and T. Arai, *Chem. Lett.*, 2005, **34**, 492–493.

5 (*a*) Y. Odo, K. Matsuda and M. Irie, *Chem.–Eur. J.*, 2006, **12**, 4283–4288; (*b*) S. H. Kawai, S. L. Gilat and J. M. Lehn, *Eur. J. Org. Chem.*, 1999, 2359–2366; (*c*) M. Irie, Y. Hirano, S. Hashimoto and K. Hayashi, *Macromolecules*, 1981, **14**, 262–267; (*d*) K. Ishihara, T. Matsuo, K. Tsunemitsu and I. Shinohara, *J. Polym. Sci., Polym. Chem. Ed.*, 1984, **22**, 3687–3695.

6 (*a*) A. Onoda, Y. Yamada, J. Takeda, Y. Nakayama, T. Okamura, M. Doi, H. Yamamoto and N. Ueyama, *Bull. Chem. Soc. Jpn.*, 2004, **77**, 321–329; (*b*) A. Onoda, Y. Yamada, Y. Nakayama, K. Takahashi, H. Adachi, T. Okamura, A. Nakamura, H. Yamamoto, N. Ueyama, D. Vyprachticky and Y. Okamoto, *Inorg. Chem.*, 2004, **43**, 4447–4455; (*c*) N. Ueyama, K. Takahashi, A. Onoda, T. Okamura and H. Yamamoto, *Macromol. Symp.*, 2003, **204**, 287–294; (*d*) D. Kanamori, T. Okamura, H. Yamamoto and N. Ueyama, *Angew. Chem., Int. Ed.*, 2005, **44**, 969–972; (*e*) D. Kanamori, A. Furukawa, T. Okamura, H. Yamamoto and N. Ueyama, *Org. Biomol. Chem.*, 2005, **3**, 1453–1459; (*f*) D. Kanamori, Y. Yamada, A. Onoda, T. Okamura, S. Adachi, H. Yamamoto and N. Ueyama, *Inorg. Chim. Acta*, 2005, **358**, 331–338; (*g*) K. Takahashi, M. Doi, A. Kobayashi, T. Taguchi, A. Onoda, T. Okamura, H. Yamamoto and N. Ueyama, *J. Cryst. Growth*, 2004, **263**, 552–563; (*h*) N. Ueyama, K. Takahashi, A. Onoda, T. Okamura and H. Yamamoto, *Macromol. Symp.*, 2002, **186**, 129–134; (*i*) N. Ueyama, H. Kozuki, M. Doi, Y. Yamada, K. Takahashi, A. Onoda, T. Okamura and H. Yamamoto, *Macromolecules*, 2001, **34**, 2607–2614; (*j*) A. Onoda, Y. Yamada, M. Doi, T. Okamura and N. Ueyama, *Inorg. Chem.*, 2001, **40**, 516–521; (*k*) A. Onoda, H. Yamamoto, Y. Yamada, K. Lee, S. Adachi, T. Okamura, K. Yoshizawa-Kumagaye, K. Nakajima, T. Kawakami, S. Aimoto and N. Ueyama, *Biopolymers*, 2005, **80**(2 and 3), 233–248; (*l*) D. Kanamori, Y. Yamada, A. Onoda, T. Okamura, S. Adachi, H. Yamamoto and N. Ueyama, *Inorg. Chim. Acta*, 2005, **358**, 85–92; (*m*) N. Ueyama, M. Inohara, A. Onoda, T. Ueno, T. Okamura and A. Nakamura, *Inorg. Chem.*, 1999, **38**, 4028–4031.

7 (*a*) T. Matsuhira, H. Yamamoto, A. Onoda, T. Okamura and N. Ueyama, *Org. Biomol. Chem.*, 2006, **4**, 1338–1342; (*b*) T. Matsuhira, H. Yamamoto, A. Onoda, T. Okamura and N. Ueyama, *Org. Biomol. Chem.*, 2008, **6**, 1926–1933.

8 A. Altomare, M. C. Burla, M. Camalli, M. Cascarano, C. Giacovazzo, A. Guagliardi and G. Polidori, *J. Appl. Crystallogr.*, 1994, **27**, 435.

9 G. M. Sheldrick, SHELXS-97, *Program for the Refinement of Crystal Structures*, University of Göttingen, Göttingen (Germany), 1997.

